Simple model for the DNA denaturation transition

Maria Serena Causo,* Barbara Coluzzi,† and Peter Grassberger‡
John von Neumann-Institut für Computing (NIC), Forschungszentrum Jülich, D-52425 Jülich, Germany
(Received 13 October 1999)

We study pairs of interacting self-avoiding walks $\{\boldsymbol{\omega}^1, \boldsymbol{\omega}^2\}$ on the $3d$ simple cubic lattice. They have a common origin $\boldsymbol{\omega}_0^1 = \boldsymbol{\omega}_0^2$, and are allowed to overlap only at the same monomer position along the chain: $\boldsymbol{\omega}_i^1 \neq \boldsymbol{\omega}_j^2$ for $i \neq j$, while $\boldsymbol{\omega}_i^1 = \boldsymbol{\omega}_i^2$ is allowed. The latter overlaps are indeed favored by an energetic gain ϵ. This is inspired by a model introduced long ago by Poland and Sheraga [J. Chem. Phys. **45**, 1464 (1966)] for the denaturation transition in DNA where, however, self avoidance was not fully taken into account. For both models, there exists a temperature T_m above which the entropic advantage to open up overcomes the energy gained by forming tightly bound two-stranded structures. Numerical simulations of our model indicate that the transition is of first order (the energy density is discontinuous), but the analog of the surface tension vanishes and the scaling laws near the transition point are exactly those of a second-order transition with crossover exponent $\phi = 1$. Numerical and exact analytic results show that the transition is second order in modified models where the self-avoidance is partially or completely neglected.

PACS number(s): 87.15.Aa, 64.60.Kw

I. INTRODUCTION

The study of the nature of the DNA denaturation is a long standing open problem. Experimentally a multistep behavior in light absorption as a function of the temperature was observed already in the 1950s (see [1] as a review). This suggested a sudden sharp opening of clusters of base pairs in cooperatively melting regions. This scenario is reminiscent of the behavior at a discontinuous first-order phase transition, in which the system changes its state from a double-strand to two molten single-stranded chains. Since then, this scenario has been verified and studied in great detail [1].

Early theoretical attempts to model this transition could not reproduce these phenomena. The first attempt with a one-dimensional Ising-like model in which the two states of spin correspond to an open or closed state of the base pair, with a favorable coupling between neighbor pairs that are in the same state [2,3], reproduced a crossover between the two different regimes but no thermodynamical transition.

The first refinement consisted in taking into account the different entropic weights of opened bubbles and double-stranded segments [4], since the phase space region that two terminally joined (but otherwise free) open strands can explore is bigger than the one accessible to a double strand of the same length.

This model was solved using the entropic weights of self-avoiding loops in Refs. [5,6]. In this way the self-avoidance between bases within the same loop is taken into account, but the other mutually excluded volume effects are completely neglected. This simplified model displayed a smooth second-order transition in two and three dimensions.

These models were, of course, only very rough caricatures of the true complexity of the problem. Even if we believe that microscopic details should be irrelevant for the existence and order of the DNA melting transitions, there are a number of aspects that one might suspect to be relevant. In addition to self-avoidance these include the stiffness of DNA, the difference in stiffness between single- and double-stranded DNA, the different properties of *A*-*T* and *C*-*G* pairs, and the helical structure of double-stranded DNA. Finally, one should also consider the effect of ''wrong'' base pairings, either between bases of the two different strands or between bases within the same strand.

There seems to exist up to now no model that incorporates all these aspects. But there have been recent models where some of them were included, and which seem to reproduce the sudden opening of base pairs. The common property in all of them is an entropic barrier that favors configurations in which base pairs are far apart.

The ''nonlinear model,'' introduced in [7,8], assumes that the stacking energy between neighboring base pairs depends on whether these pairs are in ''helical'' or ''coil'' states (i.e., whether they are bound in a double string or not). In a helix, this stacking energy is larger than in a coil. Transfer-integral calculations, molecular dynamics simulations [7], and approximate analytical methods [8] pointed out a first-order phase transition.

A recent model goes in the same direction [9], in which the helical structure is taken seriously. As a result, a mechanical torque that tends to increase or decrease the winding becomes a new thermodynamical variable. A transfer matrix calculation [10] shows that this model exhibits a first-order phase transition in the temperature-torque plain, analogous to the liquid-gas transition in the temperature-pressure plane.

Finally, according to a recent study [11], the effect of the heterogeneity in the DNA sequence—which amounts to a frozen disorder in the base pair binding strength—has no effect on the order of the transition if the model contains no entropic barrier, but it gives rise to a multistep energetic landscape if a state dependent stiffness of the type considered in [7] is introduced.

The case in which two directed polymers randomly interact has been exactly solved in Refs. [12,13] in generic di-

*Electronic address: M.S.Causo@fz-juelich.de
†Electronic address: B.Coluzzi@fz-juelich.de
‡Electronic address: P.Grassberger@fz-juelich.de

mensions. The existence of a critical dimension above which the disorder is irrelevant and a transition from a weak to a strong-disorder regime takes place has been discussed and the correlation length exponent at the transition point has been determined.

In the present paper we consider a simplified model where all these features are disregarded, but—in contrast to the papers mentioned above—excluded volume interactions are fully incorporated. Our model consists of two interacting self-avoiding walks, corresponding to the two single strands, with the same origin on a $3d$ cubic lattice. Each monomer corresponds to a base and is supposed to have its complement at the same position in the other chain. Two monomers with different positions in the two chains are not allowed to occupy the same lattice site, whereas the overlap of monomers at the same position is favored by an energetic gain ϵ that represents the binding energy. Base-pair misalignments are forbidden. We consider the homogeneous case, where all the binding energies are equal.

In our approach we focus mainly on the two conflicting tendencies of the system: the entropic gain due to the larger number of configurations accessible to the two open strands of the system on one hand and the tendency to build energetically favored links between the two strands on the other. The necessity to balance these opposite tendencies when minimizing the free energy leads to the finite-T phase transition between the high temperature swollen phase, and the low temperature phase in which finite fractions of the chains overlap.

II. MODEL

Let us define two N-step chains with the same origin on the $3d$ lattice $\boldsymbol{\omega}^1=\{\boldsymbol{\omega}_0^1,\ldots,\boldsymbol{\omega}_N^1\}$ and $\boldsymbol{\omega}^2=\{\boldsymbol{\omega}_0^2,\ldots,\boldsymbol{\omega}_N^2\}$ with $\boldsymbol{\omega}_i^k\in Z^3$ and $\boldsymbol{\omega}_0^1=\boldsymbol{\omega}_0^2=(0,0,0)$.

The Hamiltonian (or rather Boltzmann weight) that describes a configuration $(\boldsymbol{\omega}^1,\boldsymbol{\omega}^2)$ of our system is

$$e^{-H/KT}=\prod_{i\neq j}(1-\delta_{\boldsymbol{\omega}_i^1,\boldsymbol{\omega}_j^2})(1-\delta_{\boldsymbol{\omega}_i^1,\boldsymbol{\omega}_j^1})\times(1-\delta_{\boldsymbol{\omega}_i^2,\boldsymbol{\omega}_j^2})\exp\left(\frac{-\hat{\epsilon}}{kT}\sum_{i=0}^{N}\delta_{\boldsymbol{\omega}_i^1,\boldsymbol{\omega}_i^2}\right). \quad (2.1)$$

Thermodynamic properties of the system only depend on the reduced variable $\epsilon=-\hat{\epsilon}/KT$ that we will use in the following. The partition sum can therefore be written as

$$Z_N(\epsilon)=\sum_{n=0}^{N}c_{N,n}e^{\epsilon n}, \quad (2.2)$$

where n is the number of contacts, $n=\mathrm{card}\{i\,|\,\boldsymbol{\omega}_i^1=\boldsymbol{\omega}_i^2, i>0\}$, and $c_{N,n}$ is the number of distinct configurations with n contacts (notice that $\langle n\rangle/N$ is the natural order parameter). Alternatively, by introducing a fugacity z we can go over to the grand canonical ensemble with partition sum

$$G(z,\epsilon)=\sum_{N=0}^{\infty}z^N Z_N(\epsilon)=\sum_{N=0}^{\infty}\sum_{n=0}^{N}z^N c_{N,n}e^{n\epsilon}. \quad (2.3)$$

While we fix the starting point of the two polymers at a same origin, $\boldsymbol{\omega}_0^1=\boldsymbol{\omega}_0^2$, we allow the end points to wander freely in space. This is different from the Poland-Sheraga model [4], where also the end points were forced to coincide, $\boldsymbol{\omega}_N^1=\boldsymbol{\omega}_N^2$. At least in the ideal case, the presence of this constraint does not affect the order of the transition and this should be true also when the excluded volume interaction is taken into account. However the crossover scaling functions between different regimes are not the same in the two models and at the tricritical point, at which the transition takes place, different entropic exponents are found. In the excluded volume case there is also a topological subtlety: if chains are deformed continuously, nontrivial knots are forbidden if the end points never separate. In contrast, in our thermodynamical treatment any knots are allowed. But this should not have much influence either.

III. APPROXIMATE TREATMENT

The system can be represented as a sequence of M superimposed self-avoiding walks (SAWs) of length $n_1,\ldots,n_M$ $[n_k\geqslant 0$ with $n=\Sigma_k(n_k+1)-1]$, which correspond to helical domains in DNA where base pairs are bound together, which alternate with $M-1$ bubbles of lengths $p_1,\ldots,p_{M-1}(p_k\geqslant 1$; molten regions). On the lattice, they are self-avoiding polygons of length $2p_i$. The last part consists of two self-avoiding walks of lengths

$$r(\{n,p\})=N-\sum_{i=1}^{M}n_i-\sum_{j=1}^{M-1}p_j. \quad (3.1)$$

All the elements of the sequence must be mutually avoiding, that means that two monomers can occupy the same position in the space only if they occupy the same position along the chain.

If this last constraint is neglected, one can factorize the problem and write a generating function for the system in terms of the generating functions of single self-avoiding walks, polygons, and a pair of self-avoiding walks starting at the same origin. This leads to the ''almost unidimensional'' phase transitions of [4,5].

The partition sum in the fixed-N ensemble can be written as

$$Z_N=\sum_{\{n,p\}}S_{r(\{n,p\})}\prod_i W_{n_i}V_{p_i}, \quad (3.2)$$

where the sum runs over all possible partitions into helices and bubbles. $W_n=e^{\epsilon n/kT}c_n$, $V_p=\mathcal{C}_{2p}$, and $S_{r(\{n,p\})}=c_{2r(\{n,p\})}$. Here c_n is the number of self-avoiding walks of length n, while $\mathcal{C}_{2p}$ is the number of self-avoiding polygons of length $2p$. This partition sum is clearly an upper bound to the true one, since many configurations are included, which are not allowed due to self-avoidance.

The simplified problem can be easily solved in the grand canonical ensemble, i.e., by considering the generating function $G(z)=\Sigma_{N=0}^{\infty}z^N Z_N$. We find

$$G(z)=\frac{G_W^{\epsilon}(z)G_S(z)}{1-e^{\epsilon}G_W^{\epsilon}(z)G_V(z)}, \quad (3.3)$$

where $G_W^\epsilon(z)=\Sigma_{N=0}^\infty z^N W_N$, $G_V(z)=\Sigma_{N=0}^\infty z^N V_N$, $G_S(z)=\Sigma_{N=0}^\infty z^N S_N$. The critical behavior of the system is determined by the singularity of $G(z)$, which is closest to the origin, and it can be studied by using the asymptotic forms for the number of self-avoiding walks and polygons $c_N \approx \mu^N N^{\gamma-1}$, $\mathcal{C}_N \approx \mu^N N^{\alpha-2}$, where μ is the connectivity constant, which is a lattice dependent quantity. Two cases are possible: the singularity closest to the origin comes from $G_S(z)$ or from vanishing of the denominator. Let us focus on the case $d=3$. Recent estimates of the critical exponents are $\alpha=2-d\nu=0.23723(4)$ (where we used the estimate $\nu=0.58758(7)$ given in [14]) and $\gamma=1.1575\pm0.0006$ [15].

Let us denote with z_W, z_V and z_S the location of the singularities of the generating functions on the real axis. Since

$$G_W^\epsilon(z)=\sum_{N=0}^\infty \frac{(ze^\epsilon\mu)^N}{N^{1-\gamma}}, \quad G_V(z)=\sum_{N=0}^\infty \frac{(z\mu^2)^N}{(2N)^{2-\alpha}}, \quad G_S(z)=\sum_{N=0}^\infty \frac{(z\mu^2)^N}{(2N)^{1-\gamma}} \tag{3.4}$$

it appears immediately that $z_W=e^{-\epsilon}/\mu$, $z_S=1/\mu^2$, while $G_V(z)$ is finite at $z_V=z_S=1/\mu^2$ (since one has $2-\alpha>1$), but it diverges for $z>z_V$.

In the high temperature regime, i.e., $\epsilon\to0$, the singularity of G_S is the first to occur and the critical behavior is that of two self-avoiding walks. This means that the system is in the denaturated state, and the corresponding free-energy density is given by $f/KT=\ln z_S=-2\ln\mu$. This is just the entropy density of two self-avoiding walks with the same origin.

Since $G_W^\epsilon(z)$ is an increasing function of ϵ, for decreasing temperatures (increasing ϵ) the zero z_{WV} of the denominator in Eq. (3.3) decreases and finally becomes lower than z_S. The crossing point corresponds to the melting transition ϵ^*.

It can also be shown that the order of the transition is determined by the singular behavior of $G_V(z)$ in $1/\mu^2$, it depends on the value of the exponent $2-\alpha$ [5]. Since $G_W^\epsilon(z)$ is regular in $1/\mu^2$ at $\epsilon=\epsilon^*$, it plays an irrelevant role at the transition point and this is independent from the value of γ, i.e., the fact that the helical domains are self-avoiding or ideal does not affect the order of the transition. The free energy for $\epsilon\geqslant\epsilon^*$ is given by

$$f/KT=\begin{cases} -2\ln\mu+C(\epsilon-\epsilon^*)^{1/(1-\alpha)}+\ldots & \text{for} \quad 1<2-\alpha<2 \\ -2\ln\mu+C(\epsilon-\epsilon^*)+\ldots & \text{for} \quad 2-\alpha>2. \end{cases} \tag{3.5}$$

Since $2-\alpha=1.76276(6)$ [14], the approximate solution predicts a second-order phase transition.

The main approximation involved in the above treatment is that it neglects excluded volume effects that come from the mutual interactions of different bubbles, segments, and free ends. As already pointed out, this means that we overestimate the partition function, and the transition could be sharper than predicted by this simple model.

On the other hand, one can immediately use the above arguments to infer that the transition is certainly of second order in the case of interacting random walks, since $2-\alpha=3/2$ there, and there are no excluded volume effects to be taken into account. We present in the Appendix an exact analytical treatment of the ideal case. There we also evaluate numerically the melting value ϵ^*, and we study the scaling laws whose general structure will be discussed in the next section.

IV. SCALING LAWS

Again it is more easy to discuss the problem in the grand canonical ensemble, with the fugacity z conjugate to N. The limit $N\to\infty$ in the monodisperse ensemble corresponds to $z\nearrow z_c(\epsilon)$.

Values $z>z_c(\epsilon)$ only make sense after placing the system in a (large but) finite volume V. The two polymers are allowed to grow until they fill the volume with a finite nonzero density $\rho=2\langle N\rangle/V$, which remains constant in the limit $V\to\infty$. In this regime, we actually have two different phases, corresponding, respectively, to molten and undenatured (double-stranded) chains. It is intuitively clear that a nonzero density favors the presence of contacts, because contacts in our model reduce the volume occupied by the monomer pairs. Therefore one expects that the transition point between the molten and double-stranded phases takes place at a lower value of the interaction parameter $\epsilon_L^{\text{dense}}(z)$ when the fugacity z increases. This phase diagram is shown in Fig. 1.

Notice that the boundary between the molten dense phase and the short chain phase is strictly horizontal, as the attractive interaction plays no role along this transition line. Qualitatively, this phase diagram is very similar to that for a polymer attached to an adsorbing surface [16,17] and to surface transitions in magnetic systems [18]. But in contrast to the latter, the boundary between the two dense phases is not horizontal.

Using the (z,ϵ) representation, it is clear that the melting transition is a tricritical point. Its analog in magnetic systems with surfaces is the special point [18]. The curve $z=z_c(\epsilon)$ consists of two parts, a horizontal one for $\epsilon<\epsilon^*$ and a tilted one for $\epsilon>\epsilon^*$. At the melting point (z^*,ϵ^*), one sees a change of critical behavior. At finite large N, for $\epsilon<\epsilon^*$ the critical behavior of a SAW of length $2N$ is observed, while for $\epsilon>\epsilon^*$ the system displays a double-stranded behavior. At fixed N, for ϵ near ϵ^*, a crossover between the tricritical behavior and the double-stranded one ($\epsilon>\epsilon^*$) or between the tricritical behavior and the $2N$-SAWs one ($\epsilon<\epsilon^*$) is

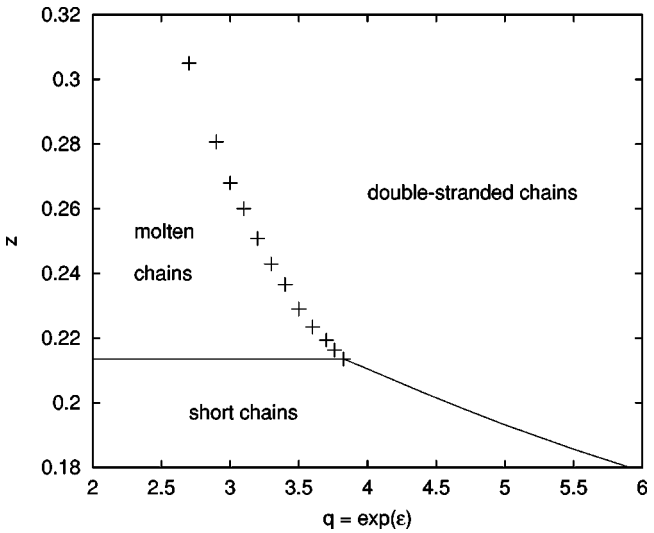

FIG. 1. Phase diagram. On the horizontal axis is plotted the Boltzmann factor $q=e^{\epsilon}$ per bound monomer pair, while the fugacity is plotted vertically. Below the continuous line, chains are short with an essentially exponential distribution in chain length. At this line, the average chain length diverges. To the left of the triple (and tricritical) point, the line is horizontal (i.e., the critical fugacity is independent of q and coincides with the value for normal SAWs). The ''molten chains'' and ''double-stranded chains'' phases are well defined only for finite volume V, with the chain length $N \propto V$. The numerical determination of the phase boundaries is discussed in Sec. VI. While the continuous line is very precise (error less than the width of the line), the uncertainty of the molten/double-stranded phase boundary is at least as big as the symbol size.

observed as ϵ tends to ϵ^*. The width of the crossover region decreases as N increases.

In the following we shall discuss the scaling laws that would be expected if the melting transition is second order. If it is first order, it seems at first not clear whether the usual scaling scenario (which is based on the existence of a divergent length scale) still holds. We shall see in Sec. VI that it does hold even then. An analytic study in the ideal case (no excluded volume) is shown in the Appendix.

Near a tricritical point, the partition sum is expected to scale as

$$G(z,\epsilon)=(z^*-z)^{-\gamma^*}F[(\epsilon-\epsilon^*)/(z^*-z)^{\phi}], \qquad (4.1)$$

with ϕ being called the crossover exponent. The scaling function $F(x)$ is nonsingular at $x=0$, from which follows

$$Z_N(\epsilon^*)\sim(1/z^*)^N N^{\gamma^*-1} \qquad (4.2)$$

for the scaling exactly at the melting point.[1]

For $\epsilon>\epsilon^*$ and $z\to z_c(\epsilon)$ from below, $G(z,\epsilon)$ must scale as the partition sum for a (double-stranded) SAW, $G\sim\text{const}/[z_c(\epsilon)-z]^{\gamma}$. Therefore $F(x)$ must have a singularity at some finite value x_0 where it diverges as

$$F(x)\sim\frac{\text{const}}{(x_0-x)^{\gamma}}, \qquad (4.3)$$

and for small $\epsilon-\epsilon^*$

$$z^*-z_c(\epsilon)\sim x_0^{-1/\phi}(\epsilon-\epsilon^*)^{1/\phi}. \qquad (4.4)$$

Thus the crossover exponent ϕ describes how the critical fugacity depends on the contact energy in the bound (nonmolten) phase.

Finally, for $\epsilon<\epsilon^*$ and $z\nearrow z^*$ we must have $G\sim\text{const}/(z^*-z)^{\gamma}$. This is the case if

$$F(x)\sim(-x)^{\sigma}, \quad x\to-\infty \qquad (4.5)$$

with some power σ, and

$$\gamma^*+\phi\sigma=\gamma. \qquad (4.6)$$

Performing the Laplace transform one checks easily that Eq. (4.1) is obtained with the ansatz

$$Z_N(\epsilon)=\mu(\epsilon)^N N^{\gamma^*-1}\Psi[(\epsilon-\epsilon^*)N^{\phi}] \qquad (4.7)$$

with $\mu(\epsilon)=1/z_c(\epsilon)$. In order to get the right asymptotics for $\epsilon\neq\epsilon^*$, the scaling function $\Psi(x)$—which is related to $F(x)$ by a Laplace transform—must scale as $|x|^{(\gamma-\gamma^*)/\phi}$ for $x\to\pm\infty$.

The scaling of the energy is obtained by differentiating Z_N with respect to ϵ. It is [16]

$$E_N(\epsilon)\sim\begin{cases}(\epsilon-\epsilon^*)^{1/\phi-1}N & \text{for } \epsilon>\epsilon^*\\ N^{\phi} & \text{for } \epsilon=\epsilon^*\\ 1/(\epsilon^*-\epsilon) & \text{for } \epsilon<\epsilon^*.\end{cases} \qquad (4.8)$$

From this we see that a first-order transition is obtained for $\phi=1$. The scaling of the specific heat is obtained by deriving once more with respect to ϵ. One finds that the peak of the specific heat scales as $N^{2\phi-1}$ and is located at $\epsilon^*+\text{const}/N^{\phi}$.

One can also look at the system from an extended scaling point of view [19–21]. We define two correlation lengths ξ_1 and ξ_2. The second, which we call the *geometrical* correlation length, is identified with the Flory radius of any of the two polymers $\xi_2=\langle(\boldsymbol{\omega}_N^1-\boldsymbol{\omega}_0^1)^2\rangle^{1/2}=\langle(\boldsymbol{\omega}_N^2-\boldsymbol{\omega}_0^2)^2\rangle^{1/2}$. It follows the scaling law $\xi_2\sim N^{\nu}$ in any phase. The first, ξ_1, is the *thermal* correlation length. It is defined as the mean diameter of the molten ''bubbles.'' In the bound phase we expect it to scale with N and $(\epsilon-\epsilon^*)$ in the same way as the end-to-end distance between the two strands, $\xi_1\propto R_{\text{end}}=\langle(\boldsymbol{\omega}_N^2-\boldsymbol{\omega}_N^1)^2\rangle^{1/2}$. If the denaturation transition is second order, the thermal correlation length ξ_1 inside the bound phase converges in the limit $N\to\infty$ to a constant that depends on ϵ, but the value of the constant diverges as $\epsilon\searrow\epsilon^*$. Exactly at $\epsilon=\epsilon^*$ it should scale as a function of N in the same way as ξ_2, i.e., both correlation lengths should be equivalent.

[1]The value of γ^* in the ideal case is computed in the Appendix. We find $\gamma^*=1+\phi$ [see Eq. (A40)]. On the other hand, if both the extremities are bound together as in the Poland-Sheraga model, it is easy to see that the crossover exponent ϕ does not change, but the absence of $G_S(z)$ in the numerator of Eq. (3.3) gives a different singular behavior at ϵ^*. It is simple to see, following the same lines as in the Appendix, that this gives $\gamma^*=\phi$.

In contrast, in a usual first-order transition we would expect that the thermal correlation length remains finite as N tends to infinity also in the limit $\epsilon \searrow \epsilon^*$, but we will see that in our system this picture does not hold because of vanishing of a surface tension. In approaching the transition point from the molten phase $R_{\rm end}$ scales as the Flory radius and is then not related to ξ_1.

Denoting with a subscript T the exponents that govern the scaling laws in the thermal parameter $\epsilon - \epsilon^*$, we can define a thermal correlation length exponent ν_T by assuming $\xi_1 \sim (\epsilon^* - \epsilon)^{-\nu_T}$ in the limit where we take first $N \to \infty$ and then $\epsilon \to \epsilon^* - 0$. One has [20,21]

$$\phi = \nu / \nu_T . \tag{4.9}$$

This can be understood in two ways. First, one can invoke the fact that $\xi_2 \sim \xi_1$ when $\epsilon = \epsilon^*$. Then Eq. (4.9) expresses just the fact that $\partial \xi^2 / \partial \epsilon$ and $\partial \xi^2 / \partial z$ are related by Eq. (4.4).

Alternatively, one observes that $D = 1/\nu$ is just the (Hausdorff) dimension of the system, whence the specific heat exponent $\alpha_T = 2 - 1/\phi$ takes the familiar hyperscaling form $\alpha_T = 2 - D\nu_T$ [21].

Let us finally discuss histogram methods that have become increasingly popular during the last years. They provide expectation values at temperatures different from those used in the simulations. In addition, they are used to study finite lattice size effects. Near an ordinary temperature-driven critical point, the energy distribution scales in a finite spin system of length L as [22,23]

$$P_L(E) \sim L^{-1/\nu} p[(E - \langle E_c \rangle)/L^{1/\nu}]. \tag{4.10}$$

This is different for a first-order transition where the distribution has two peaks that get increasingly separated when the system size is increased. The minimum between the two peaks becomes exponentially deep (with the depth controlled by the surface tension between the two phases), and the peaks become arbitrarily sharp in the limit $L \to \infty$.

Instead of studying the distribution for fixed *lattice* size, in the present case it is natural to study it for fixed finite N. In view of $E \sim N^{\phi}$, one might now expect a similar behavior

$$P_N(E) \sim N^{-\phi} p(E/N^{\phi}). \tag{4.11}$$

In Sec. VI we show that this is indeed true for the melting transition of ordinary random walks in dimensions $2 < d < 4$. There the transition is second order with $\phi = d/2 - 1$, and Eq. (4.11) is correct. But surprisingly Eq. (4.11) is also correct for ordinary random walks in dimensions $d > 4$, where $\phi = 1$ and the transition is first order. This can be understood as a vanishing of the analog of the surface tension: the cost involved in going over from a molten domain to a bound domain does not increase with N. This is obviously due to the fact that our system is (at least topologically) one dimensional. Indeed we will show in Sec. VI that the same is also true for SAW melting in $d = 3$.

We should add that histograms are particularly easy to obtain with our method of simulation (see Sec. V), since it gives us absolute estimates of partition sums. Thus combining results obtained at different nominal energies is straightforward and does not pose the problems found in Metropolis-type simulations [24]. For Fig. 5, e.g., which involved our highest statistics, we used three main runs at different temperatures, plus a number of runs with smaller statistics to sample the high-n tail.

V. SIMULATIONS

We use the pruned-enriched Rosenbluth method (PERM) [25], with Markovian anticipation [27], which is particularly effective to simulate interacting polymers [28]. In the present case the algorithm was implemented in such a way that the two chains grow simultaneously (i.e., adding one monomer to the first chain, then to the other, again to the first, and so on[2]). Following the PERM strategy, the whole system grows according to the Rosenbluth method [26] while configurations with very large/very small weight are cloned/pruned. The bias used during the Rosenbluth sampling is corrected by multiplying the weights of the configurations with the appropriate factor.

The k-steps Markovian anticipation consists in an additional bias based on the statistics of sequences of $k+1$ successive steps [27]. In dimension d, labeling by $s = 0, \ldots, 2d-1$, the $2d$ directions on a hypercubic lattice and by $S = (s_{-k}, \ldots s_0) = (\mathbf{s}, s_0)$, a given sequence of k steps ending in s_0, one considers the statistical weight $P_{N,m}(S)$ of all N-step chains, which followed the sequence S during the steps $N-m-k, \ldots, N-m$. The bias in a k-step Markovian anticipation is then given by

$$p(s_0|\mathbf{s}) = P_{N,m}(\mathbf{s}, s_0) / \sum_{s_0'=0}^{2d-1} P_{N,m}(\mathbf{s}, s_0'). \tag{5.1}$$

This means that a step in the direction s_0 is chosen more often if the previous experience tells us that it will be more successful in the far (m steps ahead) future. These biases are obviously compensated by a factor $\propto 1/p(s_o|\mathbf{s})$, to get a correct sampling. In our simulation the weights $P_{N,m}(S)$ were estimated in a preliminary run. Moreover we used an *ad hoc* bias for the present model. When the second chain has to perform a growth step and the end of the first one is in a neighboring site, we bias this step towards the end of the first chain with probability $\propto e^{\epsilon}$.

One can further increase the probability of sampling configurations with many contacts by favoring growth steps that reduce the end-to-end distance $r = |\boldsymbol{\omega}_i^2 - \boldsymbol{\omega}_i^1|$. We found that such a bias (which has to go to zero for $r \to \infty$) can substantially enhance the sampling efficiency, but leads occasionally to ''glitches'' where a disfavored configuration is encountered nevertheless, with exceptionally large weight. We therefore use only the previously described bias.

As one could expect for a first-order transition, fluctuations near ϵ^* are *very* strong, particularly on the probability distribution of the energy. A large part of our statistics was

[2]This can straightforwardly be extended to more than two chains and allows then very efficient simulations of star polymers, in particular near to collapse transitions where other methods become inefficient.

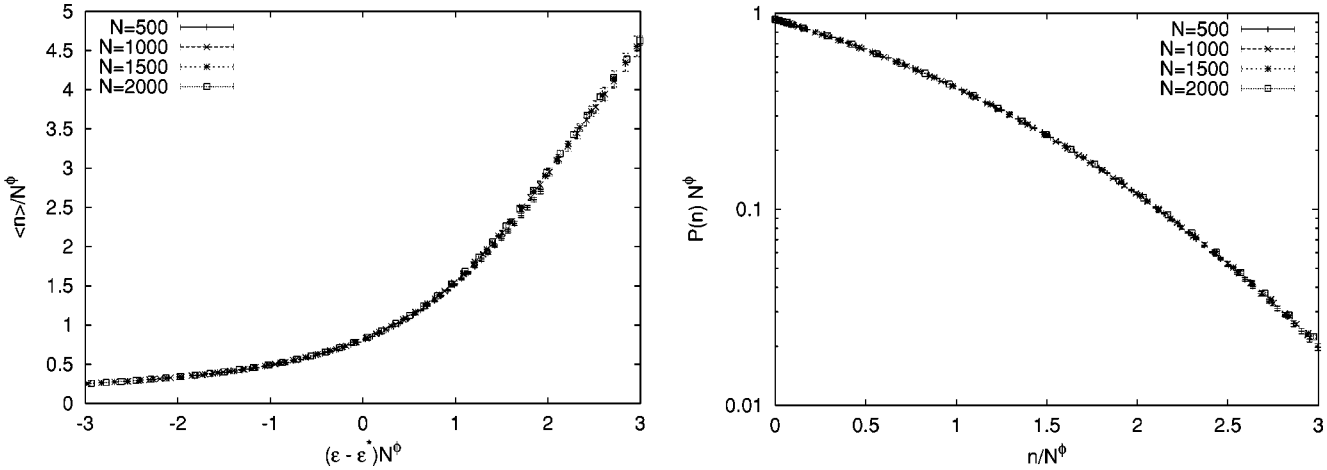

FIG. 2. Scaling plots of the average contact number for random walks in $3d$ and of the corresponding probability distribution at $\epsilon = \epsilon^*$. Here $\epsilon^* = 1.077\,26$ and $\phi = 1/2$ are the exact values (see Appendix).

collected in order to obtain clear data for $P(E)$ up to large chain lengths ($N = 3000$, i.e., a total of 6000 monomers), and for a very wide range of E. This aim was achieved by performing independent runs at five different values of the interaction strength, $\epsilon = 1.356$, 1.345, 1.343, 1.338, 1.330 and by reweighting results. At $N = 3000$ about 10^5 independent configurations were obtained for each interaction strength. The errors were evaluated with the jackknife method, i.e., by using the fluctuations between independent runs. Since we have only few such runs to compare with, the errors should be considered just as rough estimates.

Moreover we made runs up to very large chain lengths ($N = 8000$) in order to study the large-N behavior of the partition function and of the end-to-end distance. We also performed simulations at finite density (which will be discussed more in detail in the following) in order to locate the molten/double-stranded phase boundary. In all these cases the statistics was very high (typically at least 10^7 attempts or ''tours'' in the notation of [25]), but the efficiency of the method deteriorates quickly if one reaches very long chains, very low temperatures, and high densities. In contrast to usual (Metropolis-type) simulations, the problems are not due to long autocorrelations (successive tours are completely uncorrelated). Rather, in these difficult situations most tours die before reaching long chain lengths, and those which do survive have very uneven weights. Thus it might happen that even for very large samples nearly all the statistical weight is carried by one or two tours in the wings of the distribution of tour weights. Fortunately, this can be checked [29], and we are confident that this problem did not seriously affect most of our data. As for usual growth algorithms with enrichment the CPU time that the algorithm needs in order to generate an independent sample of length N grows like N^2, with an amplitude depending on the bias used [28].

As a last remark, we note that also in the ideal case in five dimensions, where it is much more simple to get good statistics, the use of a bias is necessary for correctly sampling the energy distribution in a reasonable CPU time.

VI. RESULTS AND DISCUSSION

A. The ideal case

Before discussing self-avoiding walks, we study first the case of ideal random walks, but, of course, weighting configurations with n contacts by a factor $\exp(\epsilon n)$. The study of the ideal system, which is analytically solved in the Appendix, allows us both to test the efficiency of the numerical methods and to verify the peculiar first-order transition predicted in five dimensions. We limit the analysis to simple hypercubic lattices with $d = 3$ and 5.

1. d=3

In $3d$ one finds a smooth second-order transition when moving along the solid line in Fig. 1, characterized by a value $\phi = 1/2$ of the crossover exponent. In Fig. 2(a) we plot $\langle n \rangle / N^{\phi}$ as a function of $(\epsilon - \epsilon^*) N^{\phi}$. The behavior agrees with the expected scaling law, i.e., the data are compatible with the exact values of ϵ^* and of ϕ. Furthermore, finite-size corrections appear to be small. The probability distribution $P(n)$ exactly at the critical point, properly rescaled by N^{ϕ} and plotted against n/N^{ϕ}, is shown in Fig. 2(b). The perfect data collapse confirms both the validity of the scaling law Eq. (4.11) and the efficiency of the numerical method.

2. d=5

Let us now turn on the more intriguing $5d$ case. It is shown in the Appendix that the system undergoes a first-order transition, since the contacts density $\langle n \rangle / N$ is discontinuous at ϵ^* in the thermodynamic limit, but shows scaling with a value $\phi = 1$ of the crossover exponent. We present in Fig. 3 data for $P(n)$ at the analytically calculated critical value ϵ^*. This plot is completely analogous to Fig. 2(b), but uses the exact value $\phi = 1$ (see Appendix). We see now definitely larger corrections to scaling. Also, the curves are slightly cap convex, which shows that $\langle n \rangle / N$ is not strictly discontinuous at $\epsilon = \epsilon^*$. But this is obviously a finite-size effect. For $N = 1000$, the maximum of $P(n, \epsilon)$ jumps from $n/N = 0$ to $n/N = c^* \approx 0.4$ when ϵ is increased from ϵ^* to 1.0005ϵ. In the limit $N \to \infty$, on the basis of our numerical results we can conjecture that $P(n, \epsilon^*)$ is flat between $n/N = 0$ and $n/N = c^*$.

On the other hand, it is obvious that $P(n)$ does not have the double-peak structure familiar from usual first-order transitions. In these usual cases, the valley between the peaks is due to surface tension: States with the order parameter between the two peak values contain more than one domain

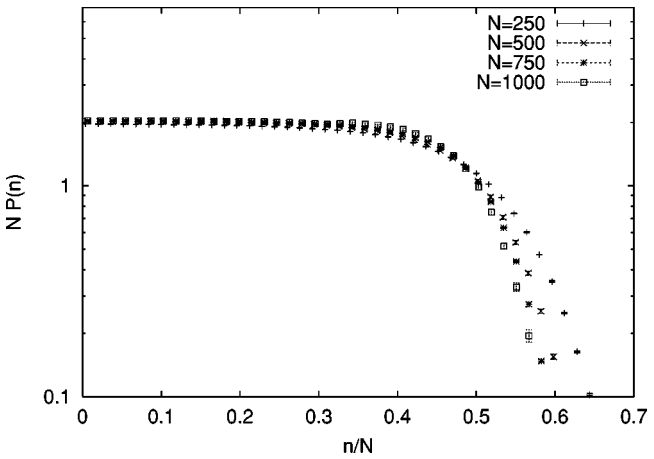

FIG. 3. Probability distribution of contact numbers for random walks in $5d$ at the exact critical value $\epsilon^* = 2.001\,15$.

and are therefore suppressed by surface tension. In the present case, there is no penalty for a transition between a molten and a double-stranded domain, explaining why all configurations with $0 \leqslant n/N \leqslant c^*$ can be equally populated (for magnetic polymers, a similar scenario was proposed recently in [30]). Notice that scaling as formulated in the previous section would not hold for usual first order transitions, since the valley between the peaks becomes exponentially deep in the thermodynamic limit, $P \sim \exp(-\sigma L^{d-1})$ for systems of linear size L. Formally, this can be reconciled with the present case by noticing that our polymers have topological dimension equal to one.

Related to this are strong fluctuations in the separation of the two chains in the double-stranded phase. Indeed, as proven in the Appendix, the average end to end distance diverges as $\xi_1 \sim (\epsilon - \epsilon^*)^{-1/2}$ as the critical point is approached from $\epsilon > \epsilon^*$. This shows that the ''thermal'' correlation length exponent is $\nu_T = 1/2 = 1/D$ and $\alpha_T = 2 - D\nu_T = 2 - \phi^{-1} = 1$.

In Fig. 4 we plot the contact number density (left panel) and the specific heat (right panel),

$$C = N^{-1}\frac{\partial E}{\partial T} = N^{-1}\epsilon^2 \frac{\partial \langle n \rangle}{\partial \epsilon} = N^{-1}\epsilon^2[\langle n^2 \rangle - \langle n \rangle^2], \tag{6.1}$$

against ϵ. In Fig.4(a), curves for different chain lengths cross nearly at the same ϵ value, which is also the value the specific heat maximum is moving towards. Within the expected uncertainty, it agrees with the predicted ϵ^*. But when trying to make the data collapse by plotting them against $(\epsilon - \epsilon^*)N^{\phi}$, we see again strong corrections to scaling. Indeed, such fits using $\langle n \rangle / N^{\phi}$ would give $\phi \simeq 0.93$ instead of $\phi = 1$. Another estimate for the crossover exponent can be recovered from the way in which the maximum of the specific heat moves toward ϵ^* as the length of the walk increases. Since in the crossover region the specific heat follows the crossover scaling, the position of the maximum for N finite is shifted by a term proportional to $N^{-\phi}$, $\phi > 1$ by a small amount. These deviations from perfect scaling give us a hint of what we have to expect when now going over to self-avoiding walks.

B. Self-avoiding walks, $d = 3$

1. Scaling of P(n) and properties derived from it

In Fig. 5 we show $\ln P(n, \epsilon^*)$, where $\epsilon^* = 1.3413 \pm 0.0004$ is our best estimate of the critical ϵ value. This distribution is clearly not convex, in contrast to the case of five-dimensional ideal random walks studied in the previous subsection. Instead, there is a peak at $n = 0$. Due to this peak, the maximum of $P(n, \epsilon)$ jumps discontinuously when ϵ passes through ϵ^* (see Fig. 6). Apart from this, the situation is very similar. We see again substantial corrections to scaling, but it seems quite clear that scaling works with $\phi = 1$. In particular, the depth of the valley between the peak at $n = 0$ and the shoulder at $n/N = c^* \approx 0.5$ does not increase with N. And, what is more important, the value of c^* does not substantially decrease with N. This is our strongest numerical evidence for the transition to be of first order. It should be noted that here we are considering quite long chains (up to $N = 3000$) and that the data for $N = 2500$ and for $N = 3000$ are nearly indistinguishable.

Deviations from the scaling behavior are seen mostly for large n/N. There, the distribution becomes increasingly steeper with N. This was seen also for ideal random walks in $d = 5$. It is indeed easy to understand. At large n, we expect $P(n) \sim e^{\epsilon n}(N/n)^n(1 - n/N)^{n-N}$, which does not follow our scaling law but is in qualitative agreement with our data.

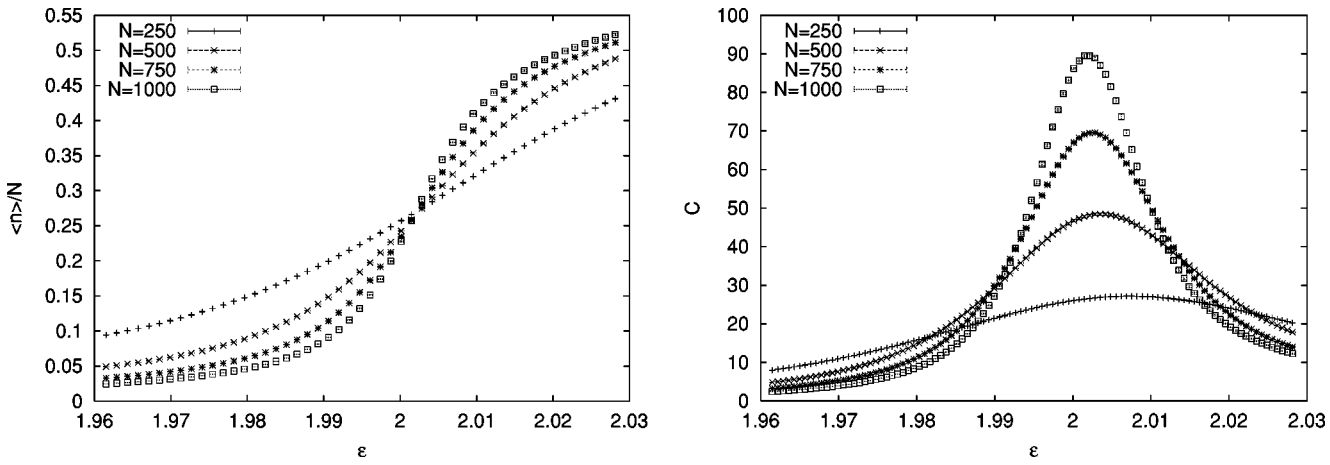

FIG. 4. Average contact number and specific heat per site for random walks in $5d$.

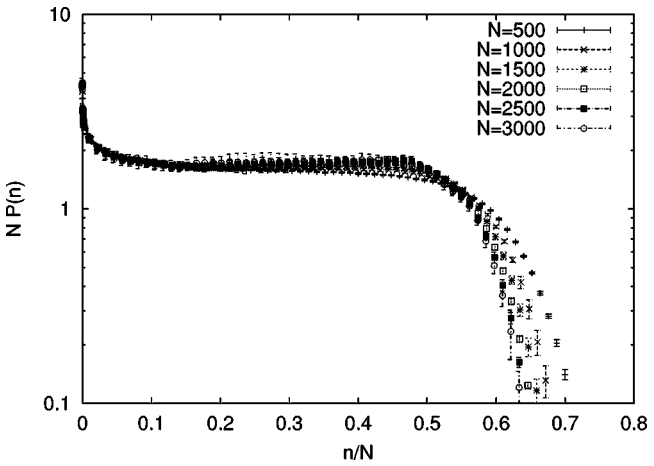

FIG. 5. Probability distribution of the contact numbers for SAWs in $3d$ at the estimated critical value $\epsilon^* = 1.3413(4)$.

Accordingly, also the scaling of $\langle n \rangle / N$ becomes poor for large ϵ, as seen from Fig. 7(b). If we try to optimize this scaling plot, we would find $\phi \approx 0.94$. But we know that this would be wrong since this would put too much emphasis on the region $n/N \approx 1$ in the contact number distribution, which we know to be not scaling.

We face a similar situation when looking at the specific heat. As seen in Fig. 8, the height of the maximum [see Fig. 9(a)] increases roughly $\propto N$, which would correspond to $\phi = 1$, but a least squares fit of our data shows an effective exponent $\phi < 1$. Since we are working with $N \leqslant 3000$, in a regime which is far from the critical one, we expect that our estimate is biased by the presence of corrections to scaling. Anyway no clear trend in the computed exponent is obtained from fits of data with cuts corresponding to increasing values of N (see Table I). All the obtained values are compatible in the statistical errors, but a χ^2 analysis indicates that our errors could be overestimated. Nevertheless the central value of the effective exponent increases with the increasing of N_{min}. This could indicate the presence of corrections to scaling. The last value obtained for $N = 1500$ is compatible with $\phi = 1$.

On the other hand, fitting the shift of the position of the maximum, which is shown in Fig. 9(b), one would get $\phi = 1.31(14)$. In this case the large statistical errors on our data do not allow any guess on the correction to scaling effects.

In summary, these results show that the melting transition for interacting SAWs in three dimensions is first order, while the analogous transition for interacting ideal walks in three dimensions is second order. This agrees with our expectation that excluded volume effects should make the transition sharper. We should add that we also performed simulations of a third version of the model, in which the two polymers were self- but not mutually avoiding (data not shown). While two monomers of the same chain were not allowed to occupy the same site, two monomers from different chains were allowed to do so, and this contributed to the energy if and only if the indices of the monomers were the same. For this intermediate model we found a $P(n)$ very similar to Fig. 5, but with a less pronounced peak at $n = 0$ and a very small nonconvex region. Therefore we are not sure whether the transition in this model is first or second order.

2. The thermal correlation length

Up to now we only looked at the scaling behavior of $P(n)$ and at quantities that are related to it straightforwardly. We mentioned already in Sec. IV several scaling, laws that are less directly related.

The most interesting ones concern the *thermal* correlation length (see Sec. IV). In the double-stranded phase ($\epsilon > \epsilon^*$) we can identify it with the rms distance $R_{\rm end}$ between the end points of the two chains. Numerical results for the latter (both for $\epsilon > \epsilon^*$ and for $\epsilon < \epsilon^*$) are shown in Fig. 10. For $\epsilon > \epsilon^*$, $R_{\rm end}$ tends for $N \to \infty$ to a constant that diverges when the tricritical point is approached, showing that there is indeed a divergent thermal correlation length, which is independent of the system size for large systems. Exactly at the tricritical point we find $R_{\rm end} \sim N^{\nu}$, showing that there the thermal and the ''geometrical'' correlation length (the Flory radius) coincide. The latter is also known from polymer adsorption to a wall, see, e.g., [16,17]. The divergence of $\xi_1 = \lim_{N \to \infty} R^2_{\rm end}$ for $\epsilon \to \epsilon^* + 0$ is shown in Fig. 11. We see that the *thermal* correlation length exponent ν_T, defined by $\xi_1 \sim (\epsilon - \epsilon^*)^{-\nu_T}$, agrees with the Flory exponent ν (the *geometrical* correlation length exponent). Since $\phi = \nu / \nu_T$ [20,21], we find again $\phi = 1$.

For $\epsilon < \epsilon^*$ we also have $R_{\rm end} \sim N^{\nu}$. But in this regime, $R_{\rm end}$ does not scale as the thermal correlation length. Instead,

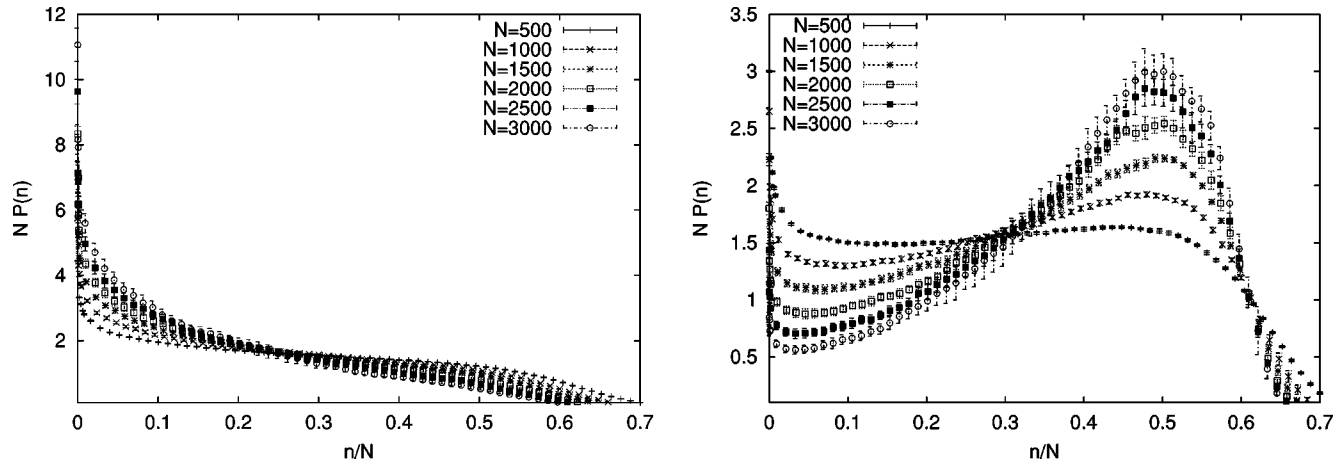

FIG. 6. Probability distribution of the contact numbers for SAWs in $3d$ at $\epsilon = 0.999\epsilon^*$ and $\epsilon = 1.001\epsilon^*$.

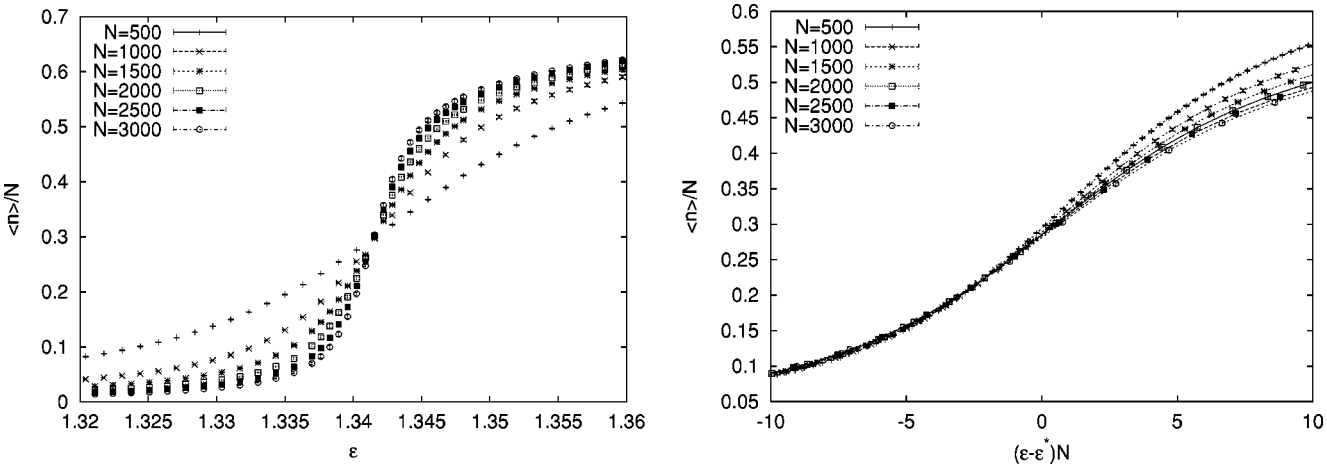

FIG. 7. The average contact number per monomer plotted against ϵ (left panel) and against $(\epsilon-\epsilon^*)N$ (right panel).

we can identify ξ_1 with the average diameter of small molten ''bubbles'' (which we did not measure since our algorithm would give very large errors). Since SAWs in three dimensions are not recurrent, large bubbles do not occur in the molten phase, and ξ_1 is finite and decreases with decreasing ϵ.

Finally, end-to-end distance distributions are shown in Fig. 12. For $\epsilon<\epsilon^*$ they coincide for large N with the end-to-end distance distributions of noninteracting SAWs of length $2N$, except for a region of very small distances, which becomes irrelevant in the limit $N\to\infty$. More precisely, if we denote with $c_N(\vec{R})$ the number of N-step walks whose end points are at a distance $R=|\vec{R}|$ apart, we have

$$f_N(x)\equiv(2d)^{-d/2}R_{\rm end}^d P_N(\vec{R})$$
$$=(2d)^{-d/2}R_{\rm end}^d\frac{c_N(\vec{R})}{\sum_{\vec{R}} c_N(\vec{R})}$$
$$\approx f(x)[1+O(N^{-\Delta})], \tag{6.2}$$

where $x=(2d)^{1/2}R/R_{\rm end}$, $f(x)$ is a universal function, and Δ is a correction to scaling exponent. As shown in [33], $f(x)$ is well approximated by a phenomenological representation given first by McKenzie and Moore [31,32]. A comparison with the latter is shown in Fig. 13. For small x the attraction between monomers is felt and $f_N(x)$ is larger than for ordinary SAWs, but this effect disappears for $N\to\infty$, as long as ϵ is strictly smaller than ϵ^*. The transition between the regimes $\epsilon>\epsilon^*$ and $\epsilon<\epsilon^*$ is not through a double-peaked distribution as one might expect for a first-order transition, but there is an approximately flat plateau at $\epsilon\approx\epsilon^*$.

3. The molten/double-stranded phase transition

The boundary between the two dense phases in Fig. 1 (crosses) was obtained by taking finite lattices of size L^3 with periodic boundary conditions. During the simulation we measured only the energy (number n of contacts) and the partition sum. The phase transition is seen as a rapid increase of $\langle n\rangle$ when the monomer density $\rho=N/L^3$ increases above a value $\rho_1(\epsilon)$. Let us define $z_1(\epsilon)$ such that

$$\frac{\partial}{\partial N}[z_1(\epsilon)^N Z_N(\epsilon)]_{N=\rho_1(\epsilon)L^3}=0. \tag{6.3}$$

If the transition were second order, $z_1(\epsilon)$ would be the critical fugacity at the considered value of ϵ. But our simulations show clearly that the transition is first order. In this case, there is a second value of the density $\rho_2(\epsilon)>\rho_1(\epsilon)$ such that the system is in the double-stranded phase when $\rho>\rho_2$, in the molten phase when $\rho<\rho_2$, and in a mixed phase in between. Equation (6.3) holds in the entire interval $\rho_1<\rho<\rho_2$.

For most values of ϵ we used $L=32$, only for $\epsilon>1.3$ ($q\geq 3.7$) we used larger lattices of size up to 64^3. Using the algorithm as described in Sec. IV we were able to see the first threshold ρ_1, but not the second one. Obviously, our algorithm is not efficient enough. Also, the increase of $\langle n\rangle$ was too slow for $\rho>\rho_1$. On the other hand, lattices of different sizes gave roughly consistent values of ρ_1. The algorithm became much more efficient when we based the ''population control'' (copying and pruning) on weight factors calculated with a larger value of ϵ than that used for evaluating average values (we used mostly $\epsilon=\epsilon^*$, but slightly larger values also worked well). This is easily understood. When the density is high enough that double-stranded configurations would be favored over molten ones, our en-

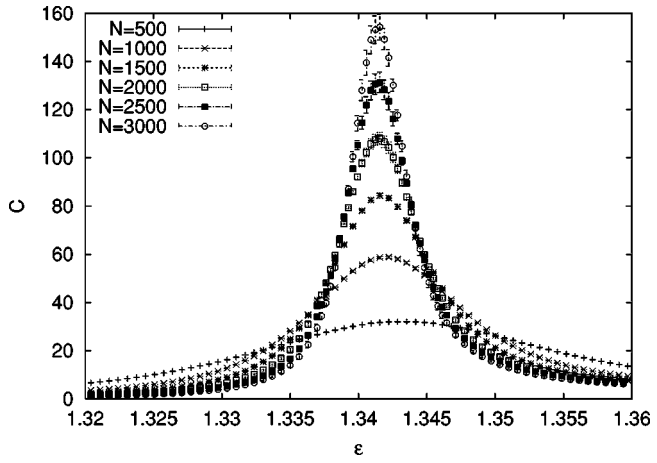

FIG. 8. The specific heat.

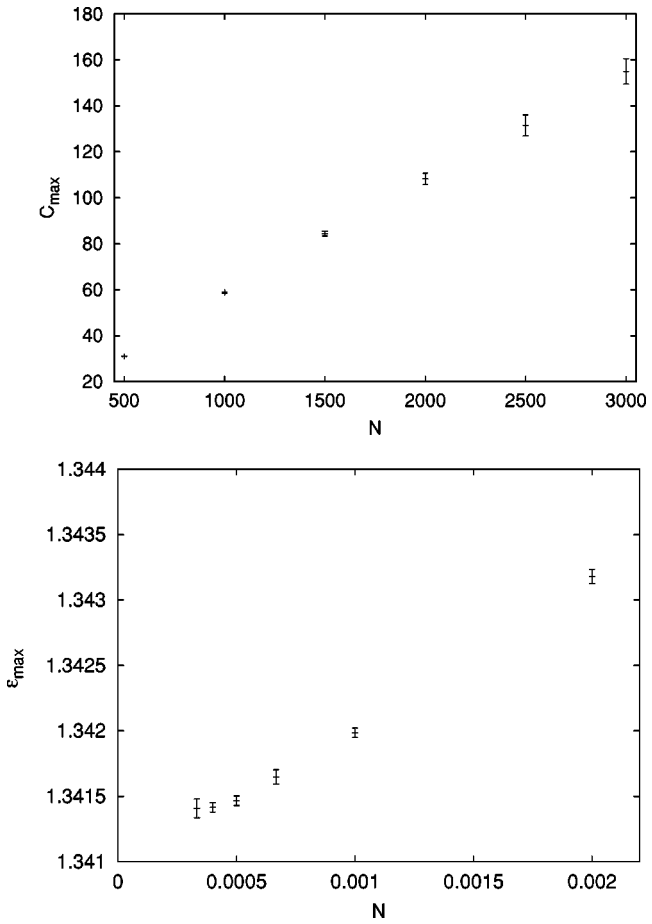

FIG. 9. The specific heat maximum and the corresponding ϵ value for SAWs in $3d$.

semble just has no such configurations, with overwhelming probability. Thus the parts of the chains grown at ambient densities $\rho > \rho_1$ are correct, but the older parts are wrong and have virtually no chance to be corrected by regrowing. This

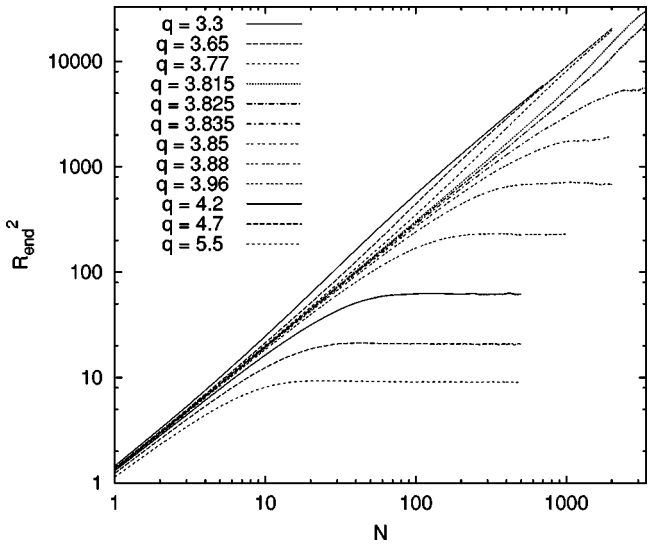

FIG. 10. Average squared end-to-end distance R_{end}^2 for various values of $q = e^{\epsilon}$, plotted against N on a double logarithmic scale. Since all curves are based on independent runs, their typical fluctuations relative to each other indicate the order of magnitude of their statistical errors.

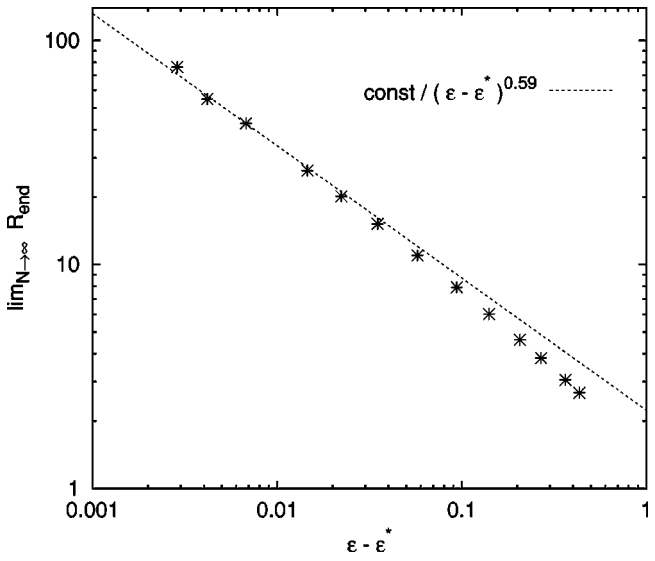

FIG. 11. Thermal correlation length $\xi_1 = \lim_{N\to\infty} R_{\text{end}}$ plotted against $\epsilon - \epsilon^*$ on a ln-ln plot. For large values of $\epsilon - \epsilon^*$, statistical errors are much smaller than the symbols. For $\epsilon - \epsilon^* < 0.01$ we cannot give exact errors, but rough estimates can be obtained by comparing with Fig. 10. The dashed line has slope -0.59, corresponding to $\nu_T = \nu$.

is no longer so when we base the population control on a higher value of ϵ. Then chains with larger n are favored already from the very beginning. As long as $\rho < \rho_1$, they will not contribute significantly because they have a tiny weight. But at $\rho > \rho_1$, their typical weight will become larger than that of the completely molten chains, and they will start to contribute. We found that $\langle n \rangle$ indeed increased very rapidly in a very narrow density interval of a few percent, when using this improved algorithm. This still did not allow us to measure reliably the difference $\rho_2 - \rho_1$, but it convinced us of the correctness of the scenario (in particular of the first

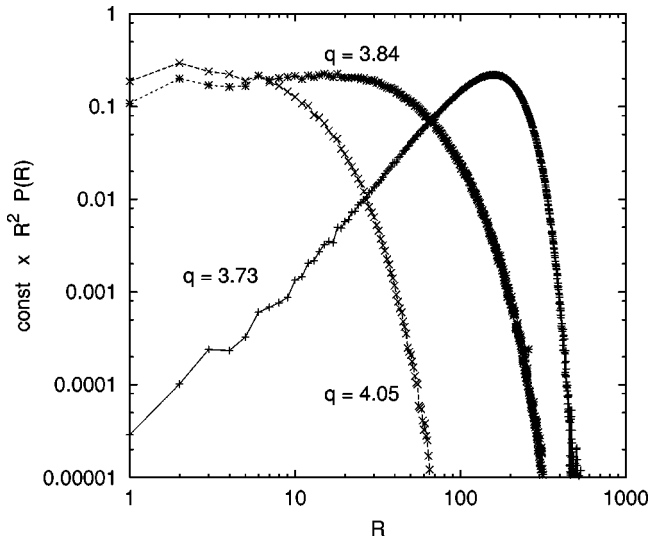

FIG. 12. Distributions of end-to-end distances at $N = 3000$ for three values of $q = e^{\epsilon}$. Normalization is arbitrary.

TABLE I. Effective crossover exponent ϕ_{eff} from the fits of the maximum of the specific heat as a function of minimum value of $N_{\min}$ considered in the fit.

$N_{\min}$	$\phi_{\text{eff}} \pm \Delta\phi_{\text{eff}}$	χ^2	DF
500	0.920 ± 0.019	0.042	3
1000	0.925 ± 0.055	0.039	2
1500	0.98 ± 0.15	0.0015	1

order of the transition), and it gave uncertainties roughly as large as the symbol sizes in Fig. 1.

4. The short chains/double-stranded phase transition

In contrast to the above, the determination of the phase boundary between the phase having only short chains and the dense phase for $\epsilon > \epsilon^*$ was straightforward. Values $z_c(\epsilon)$ were obtained by plotting $\ln Z_N(\epsilon) - (\gamma-1)\ln N + N \ln z$ against $\ln N$ and changing z until this became horizontal for large N. Several such curves are drawn in Fig. 14. Notice that we cannot expect them to be flat at small values of N, since the behavior $Z_N \sim \mu^N N^{\gamma-1}$ is expected only when the length of the (double-stranded) chain is much larger than the typical size of a molten ''bubble'' and this makes difficult the determination of the asymptotic regime. But this does not affect the uncertainty of $z_c(\epsilon) = 1/\mu$ in a dramatic way, since Z_N is extremely sensitive to even tiny changes of μ. As a result we cannot give formal error estimates, but they are definitely smaller than $\pm 0.000\,05$. This number refers to $\epsilon \approx \epsilon^*$ where errors are largest, for $\epsilon \gg \epsilon^*$ our estimates are indeed much more precise. A blow up of this phase boundary is shown in Fig. 15. From that we verify that the boundary terminates at (ϵ^*, z^*) with finite nonzero slope, showing again that $\phi = 1$. For very large values of ϵ we see also that $[\mu(\epsilon)]^2 e^{\epsilon} \to \mu(0)$ as we should expect for a very tightly bound double-stranded chain.

From the curves with $\epsilon \approx \epsilon^*$ in Fig. 14 we can read off the exponent γ^* controlling the partition sum exactly at the tri-

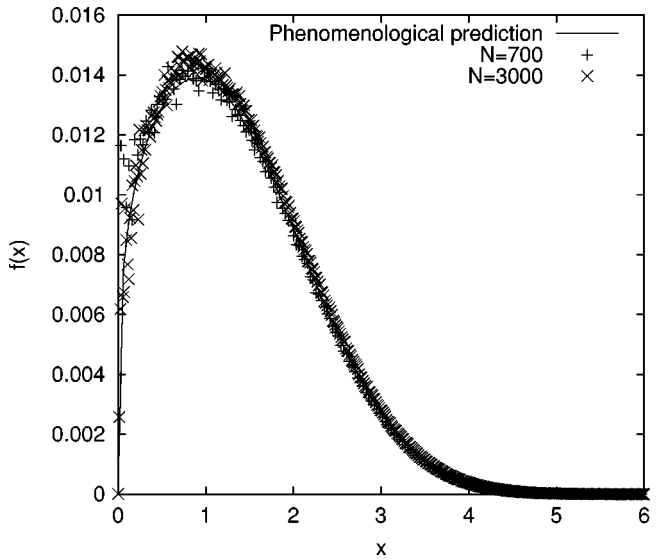

FIG. 13. Comparison of the scaling functions $f_N(x)$ for $N = 700$, $\epsilon = 1.19$ and $N = 3000$, $\epsilon = 1.32$ with the phenomenological prediction for $f(x)$ of [31,32].

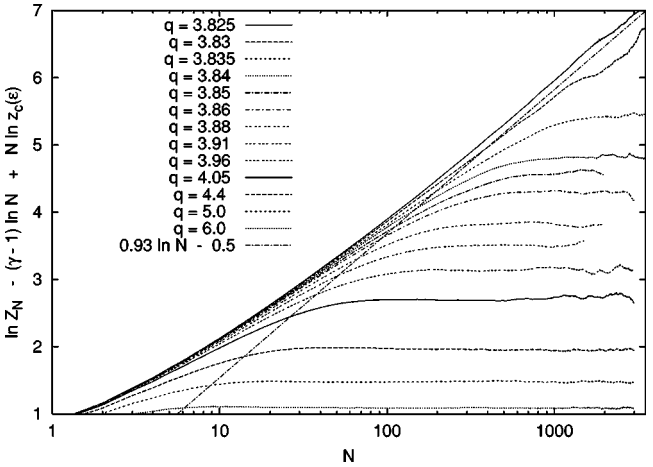

FIG. 14. Logarithms of partition sums at different values of $q = e^{\epsilon}$, after subtracting suitable terms so that they become flat for $N \to \infty$ and $\epsilon > \epsilon^*$. The straight dashed line has slope $\gamma^* - \gamma = 0.93$.

critical point. In view of the substantial finite-size corrections at small N and the uncertainties at large N due to statistical errors and the uncertainty in the exact value of ϵ^*, we obtain a rather crude estimate

$$\gamma^* = 2.09 \pm 0.1. \tag{6.4}$$

Unfortunately, we do not have any prediction for γ^* to compare this with. But for ideal random walks we have $\sigma_{rw} = -1$ (see Appendix), where σ was defined in Sec. IV and is related to γ^* by Eq. (4.6). Trying $\sigma = \sigma_{rw}$ as a first guess, we would predict $\gamma^* = 2.16$ in surprisingly good agreement with our direct estimate.

Finally, we can read off from Fig. 14 values of the function $A(\epsilon)$ in the scaling ansatz

$$Z_N(\epsilon) \simeq A(\epsilon)\mu(\epsilon)^N N^{\gamma-1}. \tag{6.5}$$

According to Eq. (4.7), this function should scale as $A(\epsilon) \sim (\epsilon - \epsilon^*)^{\gamma - \gamma^*}$. This was reasonably well satisfied.

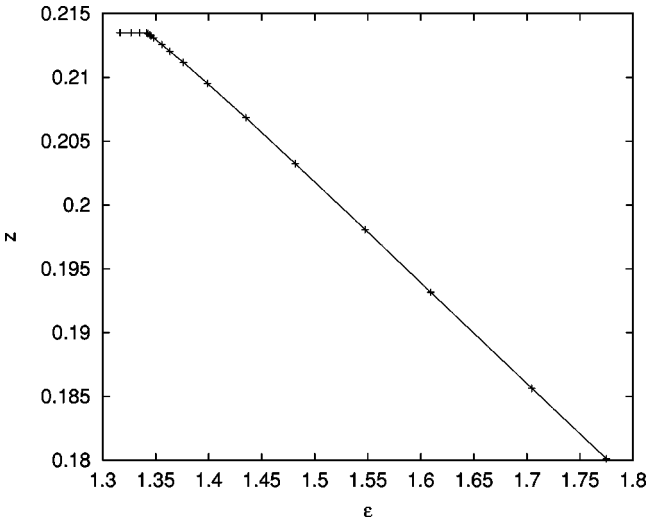

FIG. 15. Phase boundary between the short chain and double-stranded phases.

VII. CONCLUSION

We studied a simplified model for DNA denaturation. It can be considered as a lattice realization of the Poland-Sheraga model [4,5], however taking into account correctly all excluded volume effects. The melting transition in this model is simply related to the balance between the entropic gain of the two DNA strands when being independent, to be compared with the energy gain in configurations where they are tightly bound together.

The numerical results show that excluded volume effects are relevant in this transition. They change the transition from being second order (without excluded volume effects) to being first order. In spite of the latter, we find a divergent length scale, and scaling relations typical for a (tri-)critical point. We explain this by the absence of a significant surface tension between the molten and bound phases.

The present study systematically takes into account excluded volume effects in DNA melting. We have neglected a number of other features that might be equally or even more important. We plan to consider some of these in future work, which includes, in particular, heterogeneity of the chain due to the quenched sequence of DNA bases.

ACKNOWLEDGMENTS

We thank Sergio Caracciolo, Walter Nadler, Andrea Pelissetto, and Lothar Schäfer for discussions and for carefully reading the manuscript.

APPENDIX: EXACT RESULTS FOR INTERACTING IDEAL RANDOM WALKS

In this Appendix we provide an analytic solution for our model in the ideal case, i.e., when the excluded volume interaction is fully neglected, on (hyper-)cubic d-dimensional lattices. In this case the generating function can be easily computed and the order of the transition can be easily determined in any dimension. Let us define $c^{\epsilon}_{2N}(\mathbf{x})$ as the unnormalized weight of the configuration of two N-step random walks $\{\omega^1,\omega^2\}$ starting both at the origin and ending at a distance vector $\mathbf{x}=\boldsymbol{\omega}^2_N-\boldsymbol{\omega}^1_N$ apart. A step towards the same lattice position ($\mathbf{x}=0$) is favored by an energetic gain $-\epsilon$, corresponding to a Boltzmann weight e^{ϵ} (the energy is here expressed in kT units). We can then write the following recursion relation:

$$c^{\epsilon}_{2N}(\mathbf{x})=\sum_{i=1}^{d}\sum_{j=1}^{d}[c^{\epsilon}_{2N-2}(\mathbf{x}+\mathbf{e}_i+\mathbf{e}_j)+c^{\epsilon}_{2N-2}(\mathbf{x}+\mathbf{e}_i-\mathbf{e}_j)+c^{\epsilon}_{2N-2}(\mathbf{x}-\mathbf{e}_i+\mathbf{e}_j)+c^{\epsilon}_{2N-2}(\mathbf{x}-\mathbf{e}_i-\mathbf{e}_j)]\times[1+(e^{\epsilon}-1)\delta_{\mathbf{x},0}]. \tag{A1}$$

Equation (A1) suggests another interpretation. We can choose the origin of our system to coincide at any time step with the position of one of the two walkers. In this way the problem is mapped in a single random walker moving at ''double speed'' (i.e., making two random steps on the lattice at each time step). We use here the obvious fact that a walk on a hypercubic lattice can return to the origin only after an even number of steps (or that the sublattice with even parity is still a hypercubic lattice). This would not be true, e.g., for the triangular lattice.

If we denote with $c^{\epsilon}_{N}(\mathbf{x})$ the weight of the single walker configuration, the recursion relation (A1) is equivalent to

$$c^{\epsilon}_{N}(\mathbf{x})=\sum_{i=1}^{d}[c^{\epsilon}_{N-1}(\mathbf{x}+\mathbf{e}_i)+c^{\epsilon}_{N-1}(\mathbf{x}-\mathbf{e}_i)][1+(e^{\epsilon}-1)\delta_{\mathbf{x},0}], \tag{A2}$$

but because of the rescaling of time only an even number of steps corresponds to the original system.

Introducing the generating function in the grand canonical ensemble by a Laplace transform

$$G^{\epsilon}(\mathbf{x},z)=\sum_{N=0}^{\infty}c^{\epsilon}_{N}(\mathbf{x})z^N, \tag{A3}$$

one can write the Fourier transform $\hat{G}(\mathbf{q},z)$ in terms of the free propagator of the Gaussian model on the lattice

$$D(\mathbf{q},z)=\frac{1}{m_0^2+\hat{\mathbf{q}}^2}, \tag{A4}$$

where $m_0^2=(1-2dz)/z$ and $\hat{q}_i=2\sin q_i/2$, in the following way

$$\hat{G}^{\epsilon}(\mathbf{q},z)=\frac{D(\mathbf{q},z)}{ze^{\epsilon}+(1-e^{\epsilon})\int[dq]^d D(\mathbf{q},z)}, \tag{A5}$$

where the integration is done on the first Brillouin zone. The knowledge of the singular behavior in z in the small-q region in Eq. (A5) makes it possible to determinate the critical properties of the system in the monodisperse ensemble by an inverse Laplace transform.

For instance, the partition sum $Z^{\epsilon}_{2N}=\Sigma_{\mathbf{x}}c^{\epsilon}_{2N}(\mathbf{x})$, the mean value of powers of components of the square distance from the origin (or in the original system of the square distance of the two walkers) $\langle x_k^{2m}\rangle\equiv[\Sigma_{\mathbf{x}}x_k^{2m}c^{\epsilon}_{2N}(\mathbf{x})]/Z^{\epsilon}_{2N}$, and the average number of contacts $\langle n\rangle=\partial\ln(Z^{\epsilon}_{2N})/\partial\epsilon$ can be obtained by inverse transformation from the following quantities:

$$\hat{G}^{\epsilon}(0,z)=\sum_{\mathbf{x}}\sum_{N=0}^{\infty}z^N c^{\epsilon}_{N}(\mathbf{x}), \tag{A6}$$

$$(-1)^m\frac{\partial\hat{G}^{\epsilon}(\mathbf{q},z)}{\partial q_k^{2m}}\bigg|_{\mathbf{q}=0}=\sum_{\mathbf{x}}\sum_{N=0}^{\infty}z^N x_k^{2m}c^{\epsilon}_{N}(\mathbf{x}), \tag{A7}$$

$$\frac{\partial\hat{G}^{\epsilon}(0,z)}{\partial\epsilon}=\sum_{\mathbf{x}}\sum_{N=0}^{\infty}z^N\frac{\partial c^{\epsilon}_{N}(\mathbf{x})}{\partial\epsilon}. \tag{A8}$$

Because of the isotropy of the system, we write $\langle x_k^{2m}\rangle=\langle x^{2m}\rangle$. If there were no interaction ($\epsilon=0$), the critical behavior of the system would arise in the limit $m_0^2\to 0$, corresponding to $z^*=1/2d$. We are interested in changes with respect to this critical behavior due to the interaction with the origin.

It is immediately clear that a critical behavior that is different from that of free random walks case can appear in two cases: If the denominator in Eq. (A5) either vanishes or diverges at $z \leqslant z^*$. The properties of the denominator are deeply connected to the ones of the integral of the free propagator, $H(z)$.

It is easy to see that

$$H(z)=\int [dq]^d D(\mathbf{q},z) \sim \begin{cases} (m_0^2)^{d/2-1} & \text{for } d<2 \\ \ln m_0^2 & \text{for } d=2 \\ \text{finite} & \text{for } d>2 \end{cases} \tag{A9}$$

so that the case in which the critical behavior is modified because of divergencies in the denominator at $z=z^*$ can arise only for $d \leqslant 2$.

A critical behavior that characterizes a collapsed (double-stranded) phase arises when the relation

$$\frac{H[z_c(\epsilon)]}{z_c(\epsilon)}=\frac{1}{1-e^{-\epsilon}} \tag{A10}$$

can be satisfied for $z_c<z^*$, while an unstable fixed point is reached when Eq. (A10) is satisfied for $z_c=z^*$ and the singularity due to the interaction with the origin merges with the one of the free propagator.

We observe that $H(z)/z$ is an increasing function of z and that $\lim_{z\to 0} H(z)/z=1$.[3] For this reason, the above equation has no solution for $\epsilon<0$, the case of repulsive interaction. But in the region $\epsilon \geqslant 0$ one can find a critical value ϵ^* for which Eq. (A10) is satisfied for $z_c(\epsilon^*)=z^*$, with z^* defined above. For $\epsilon>\epsilon^*$ the position of $z_c(\epsilon)$ in Eq. (A10) moves closer to the origin, and $\lim_{\epsilon\to\infty} z_c(\epsilon)=0$. The point (ϵ^*,z^*) is tricritical in the sense of having codimension 2 (two control parameters have to be adjusted to obtain it). Equation (A10) gives the critical value ϵ^* on the cubic lattice, which was used in Sec. VI A

$$\epsilon^*=-\ln\left[1-2\ dH\left(\frac{1}{2d}\right)\right]. \tag{A11}$$

Three kinds of critical behavior in z can be identified in any dimension d, the one for $(\epsilon<\epsilon^*, z=z^*)$ in which the denominator in (A5) does not vanish (molten phase), the one in the *double-stranded* phase governed by $[\epsilon>\epsilon^*, z=z_c(\epsilon)]$, and the one at the tricritical point (ϵ^*,z^*), but the behavior in the different regimes depends on the dimensionality.

(i) $d \leqslant 2$. From geometrical arguments it is easy to see that when the dimension of the space is smaller than the Hausdorff dimension of the walk ($d_H=1/\nu=2$) the probability that the walker intersects a given point is finite. In this case the interaction with the origin results in a relevant perturbation that brings the system out of the universality class of the unperturbed case, as it appears from the critical behavior for $m_0^2 \to 0$ of $H(z)$. The case $d=2$ in which the dimension of the space is equal to the dimension of the walk corresponds to a marginal interaction and logarithmic corrections appear in the scaling laws. Equation (A10) has a solution $z_c(\epsilon)<z^*$ for all values of $\epsilon>0$, and $z_c(\epsilon)\to 0$ when $\epsilon\to+\infty$. This means that in the attractive regime the free propagator *always* stays finite when the denominator vanishes. In other words, there is *no transition between two different regimes when the temperature is changed if the interaction is attractive*. The system is in the double-stranded phase (or collapsed onto the origin in the other view). On the other hand, we can identify a phase transition when the sign of the interaction changes, namely at $\epsilon^*=0$, and we will show that it is a second-order one.

(ii) $d>2$. In dimension $d>2$ the presence of a zero-dimensional region that couples with the random walk introduces an irrelevant operator. The integral $H(z)$ takes a finite value and its expansion around the singularity z^* of the free propagator has the form [34]

$$H(z)=\sum_{n=0}^{\infty} A_n m_0^{2n}+C(m_0^2)m_0^{d-2}, \quad m_0^2=(1-z/z^*)/z, \tag{A12}$$

where A_n are suitable constants and $C(m_0^2)$ is a function of m_0^2, which is finite for $m_0^2\to 0$, for d odd and diverges logarithmically for d even. The leading term in $H(z)-H(z^*)$ for dimension $d<4$ is given by the nonanalytic one $C(m_0^2)m_0^{d-2}$, it is $m_0^2\ln(m_0^2)$ for $d=4$, and for $d>4$ it is given by the analytic term m_0^2. We will show that this gives rise to a change in the order of the transition when $d=4$ is crossed.

1. Molten phase

In $d>2$, for $\epsilon<\epsilon^*$ the critical behavior in the generating function is governed by the free propagator $D(\mathbf{q},z)$ whose behavior around z^* gives rise to the usual critical exponents of the random walk, but with amplitudes depending on ϵ. One can rewrite near the critical point

$$\hat{G}^{\epsilon}(\mathbf{q},z)\approx \frac{D(\mathbf{q},z)}{z^* e^{\epsilon}+(1-e^{\epsilon})H(z^*)} \tag{A13}$$

and, from the small q critical behavior of $\hat{G}^{\epsilon}(\mathbf{q},z)$ and of its derivatives with respect to q and ϵ, one can obtain the following scaling forms for large fixed N:

Partition sum,

$$Z_{2N}^{\epsilon}\approx \frac{z^*}{z^* e^{\epsilon}+(1-e^{\epsilon})H(z^*)} z^{*-2N}; \tag{A14}$$

free energy per base pair,

$$f=\lim_{N\to\infty}\frac{1}{N}\ln Z_{2N}^{\epsilon}=\ln z^{*2}, \tag{A15}$$

base-pair separation moment,

$$\langle x^{2m}\rangle \approx (2m-1)!!\, z^{*m} 4^m N^m; \tag{A16}$$

average number of contacts,

[3] The assertion follows immediately from $H(z)/z=\Sigma_{N=0}^{\infty} z^N c_N^{\epsilon=0}(0)$.

$$\langle n\rangle \approx \frac{e^{\epsilon}[H(z^*)-z^*]}{z^* e^{\epsilon}+(1-e^{\epsilon})H(z^*)}. \tag{A17}$$

In the limit $\epsilon \to \epsilon^{*-}$ the mean number of contacts $\langle n\rangle$ and the amplitude of Z_{2N}^{ϵ} diverges

$$Z_{2N}^{\epsilon} \approx \frac{z^*}{e^{\epsilon^*}[H(z^*)-z^*]}(\epsilon^*-\epsilon)^{-1} z^{*-2N}, \tag{A18}$$

$$\langle n\rangle \approx (\epsilon^*-\epsilon)^{-1}. \tag{A19}$$

For $d \leqslant 2$, instead, the singular behavior of $H(z)$ near z^* plays a role in the molten phase. For $\epsilon < \epsilon^* = 0$, near the singular region one has

$$\hat{G}^{\epsilon}(\mathbf{q},z) \approx \frac{D(\mathbf{q},z)}{(1-\epsilon)H(z)} \tag{A20}$$

and the above scaling laws become

$$Z_{2N}^{\epsilon} \sim \begin{cases} (1-e^{\epsilon})^{-1} z^{*-2N} N^{d/2-1} & \text{for } d=1 \\ (1-e^{\epsilon})^{-1}[\ln N]^{-1} z^{*-2N} & \text{for } d=2, \end{cases} \tag{A21}$$

$$f = \ln(z^{*2}), \tag{A22}$$

$$\langle n\rangle \sim \frac{1}{e^{-\epsilon}-1}, \tag{A23}$$

$$\langle x^{2m}\rangle \sim N^m \tag{A24}$$

from which the behavior for $\epsilon \to 0^-$ can be easily recovered.

2. Double-stranded phase

Let us now study the collapsed phase $\epsilon > \epsilon^*$. The denominator determines the critical behavior, since it vanishes for $z_c(\epsilon) < z^*$, where the small q behavior of $D(\mathbf{q},z)$ is not singular. Near the critical region the generating function can be rewritten as

$$\hat{G}^{\epsilon}(\mathbf{q},z) \approx \frac{D(\mathbf{q},z)}{K(\epsilon) z_c(\epsilon)[1-z/z_c(\epsilon)]} \tag{A25}$$

where $K(\epsilon) = (e^{\epsilon}-1)\partial H/\partial z|_{z_c(\epsilon)} - e^{\epsilon}$ is positive. The derivative with respect to ϵ of (A5) in the same limit reads

$$\frac{\partial \hat{G}^{\epsilon}(\mathbf{q},z)}{\partial \epsilon} \approx \frac{e^{\epsilon}\{H[z_c(\epsilon)]-z_c(\epsilon)\}}{z_c(\epsilon)^2 K^2(\epsilon)[1-z/z_c(\epsilon)]^2} D(\mathbf{q},z). \tag{A26}$$

In the same way as the previous relations for the observables have been recovered, one finds that

$$Z_{2N}^{\epsilon} \approx \frac{z_c(\epsilon)^{-2N}}{K(\epsilon)[1-z_c(\epsilon)/z^*]}, \tag{A27}$$

$$f = \ln[z_c(\epsilon)^2], \tag{A28}$$

$$\langle x^{2m}\rangle \approx (2m-1)!!\, m! \frac{z_c(\epsilon)^m}{[1-z_c(\epsilon)/z^*]^m}, \tag{A29}$$

$$\langle n\rangle \approx \frac{e^{\epsilon}\{H[z_c(\epsilon)]-z_c(\epsilon)\}}{z_c(\epsilon)K(\epsilon)} N. \tag{A30}$$

It is interesting to study the limit $\epsilon \to \epsilon^{*+}$, whose comparison with $\epsilon \to \epsilon^{*-}$ gives the order of the transition. The behavior of the denominator near ϵ^* and the way in which $z_c(\epsilon)$ approaches ϵ^* will be crucial.

We have to distinguish different cases with respect to the dimensionality of the space. Let us start with $d > 2$. From Eq. (A9) it follows that

$$ze^{\epsilon^*} + (1-e^{\epsilon^*})H(z) \sim (1-e^{\epsilon^*}) \begin{cases} (1-z/z^*)^{d/2-1} & \text{for } 2<d<4 \\ (1-z/z^*)\ln(1-z/z^*) & \text{for } d=4 \\ (1-z/z^*) & \text{for } d>4. \end{cases} \tag{A31}$$

From this relation it is a simple matter to get the behavior of $z^* - z_c(\epsilon)$ and $K(\epsilon)$ for $\epsilon \gtrsim \epsilon^*$

$$z^* - z_c(\epsilon) \sim \begin{cases} (\epsilon-\epsilon^*)^{2/(d-2)} & \text{for } 2<d<4 \\ (\epsilon-\epsilon^*)[\ln(\epsilon-\epsilon^*)]^{-1} & \text{for } d=4 \\ (\epsilon-\epsilon^*) & \text{for } d>4, \end{cases} \tag{A32}$$

$$K(\epsilon) \sim \begin{cases} (\epsilon-\epsilon^*)^{(d-4/d-2)} & \text{for } 2<d<4 \\ \ln(\epsilon-\epsilon^*) & \text{for } d=4 \\ \text{constant} & \text{for } d>4. \end{cases} \tag{A33}$$

The shift exponent ψ, defined by

$$z_c(\epsilon) = z^*[1-k(\epsilon-\epsilon^*)^{1/\psi}], \tag{A34}$$

with k constant, can be read from the above relations (A32) as a function of d. Introducing the crossover exponent ϕ

$$\phi = \begin{cases} \dfrac{d-2}{2} & \text{for } 2<d\leqslant 4 \\ 1 & \text{for } d>4, \end{cases} \tag{A35}$$

the above relations can be rewritten in a more compact form, namely, $z^* - z_c(\epsilon) \sim (\epsilon-\epsilon^*)^{1/\phi}$, $K(\epsilon) \sim (\epsilon-\epsilon^*)^{(\phi-1)/\phi}$, both with the appropriate logarithmic correction in $d=4$. One can observe that ϕ coincides with the shift exponent ψ. It follows that for $\epsilon \gtrsim \epsilon^*$,

$$Z_{2N}^{\epsilon} \approx \frac{z_c(\epsilon)^{-2N}}{\epsilon-\epsilon^*}, \tag{A36}$$

$$f \approx \ln(z^{*2}) + a \begin{cases} (\epsilon-\epsilon^*)^{1/\phi} & \text{for } d \neq 4 \\ (\epsilon-\epsilon^*)[\ln(\epsilon-\epsilon^*)]^{-1} & \text{for } d=4, \end{cases} \tag{A37}$$

$$\langle x^{2m}\rangle \approx (2m-1)!! \times m! \begin{cases} (\epsilon-\epsilon^*)^{-m/\phi} & \text{for } d\neq 4 \\ [\ln(\epsilon-\epsilon^*)]^m(\epsilon-\epsilon^*)^{-m} & \text{for } d=4, \end{cases} \tag{A38}$$

$$\langle n\rangle \approx e^{\epsilon^*}\left[\frac{H(z^*)}{\beta^*}-1\right] N \begin{cases} (\epsilon-\epsilon^*)^{(1-\phi)\phi} & \text{for } d\neq 4 \\ [\ln(\epsilon-\epsilon^*)]^{-1} & \text{for } d=4. \end{cases} \tag{A39}$$

From (A12) one sees immediately that the free energy has a discontinuity in its first derivative if $d>4$, i.e., the transition is a first-order one.

On the other hand, a different critical behavior is expected at the critical point $\epsilon=\epsilon^*$. In this special point the denominator vanishes exactly at $z_c(\epsilon)=z^*$, the point in which the free propagator has the small q singularity. The behavior of the denominator of $\hat{G}^{\epsilon^*}(\mathbf{q},z)$, its derivatives with respect to q and $\partial_\epsilon \hat{G}^{\epsilon}(\mathbf{q},z)|_{\epsilon^*}$ for z near to z^*, can be read from the asymptotic expansion in (A31).

Using the same exponent ϕ defined above, the following scaling laws hold:

$$Z_{2N}^{\epsilon^*} \sim \begin{cases} z^{*-2N}N^{\phi} & \text{for } d\neq 4 \\ z^{*-2N}N^{\phi}[\ln N]^{-1} & \text{for } d=4, \end{cases} \tag{A40}$$

$$\langle x^{2m}\rangle \sim \frac{(2m-1)!!m!\Gamma(1+\phi)z^{*m}}{\Gamma(m+1+\phi)} 4^m N^m, \tag{A41}$$

$$\langle n\rangle \sim \begin{cases} N^{\phi} & \text{for } d\neq 4 \\ N^{\phi}[\ln N]^{-1} & \text{for } d=4. \end{cases} \tag{A42}$$

The case $d\leqslant 2$ can be handled in a similar way knowing the behavior of $H(z)$ near to z^*. The way in which $z_c(\epsilon)$ approaches z^* and $K(\epsilon)$ diverges when $\epsilon\to 0$ is given by

$$[z^*-z_c(\epsilon)] \sim \begin{cases} \epsilon^{2/(2-d)} & \text{for } d=1 \\ e^{-a/\epsilon} & \text{for } d=2, \end{cases} \tag{A43}$$

$$K(\epsilon) \sim \begin{cases} \epsilon^{-2/(2-d)} & \text{for } d=1 \\ e^{a/\epsilon}\epsilon & \text{for } d=2, \end{cases} \tag{A44}$$

with a positive constant. It follows that the above observables in the limit $\epsilon\to 0^+$ behave as

$$Z_{2N}^{\epsilon} \sim \begin{cases} z^{*-2N} & \text{for } d=1 \\ z^{*-2N}\epsilon^{-1} & \text{for } d=2, \end{cases} \tag{A45}$$

$$f \approx \ln(z^{*2}) + c \begin{cases} \epsilon^2 & \text{for } d=1 \\ e^{-a/\epsilon} & \text{for } d=2, \end{cases} \tag{A46}$$

$$\langle n\rangle \approx N \begin{cases} \epsilon & \text{for } d=1 \\ e^{-a/\epsilon}\epsilon^{-2} & \text{for } d=2. \end{cases} \tag{A47}$$

Taking the limit $\epsilon\to 0^+$ in Eq. (A46) and $\epsilon\to 0^-$ in Eq. (A22) it is a simple matter to see that the transition is a second-order one.

It is a simple matter to see the behavior at the tricritical point. $\hat{G}^0(\mathbf{q},z)$ becomes the free-generating function and the scaling laws that appear are the usual ones. The number of contacts can be simply recovered from the derivative of (A5) with respect to ϵ setting $\epsilon=0$. This gives the well known result

$$\langle n\rangle \sim \begin{cases} N^{1/2} & \text{for } d=1 \\ \ln N & \text{for } d=2. \end{cases} \tag{A48}$$

[1] R.M. Wartell and A.S. Benight, Phys. Rep. **126**, 67 (1985).
[2] B.H. Zimm and J.K. Bragg, J. Chem. Phys. **31**, 526 (1959).
[3] B.H. Zimm, J. Chem. Phys. **33**, 1349 (1960).
[4] D. Poland and H.A. Sheraga, J. Chem. Phys. **45**, 1456 (1966); **45**, 1464 (1966).
[5] M.E. Fisher, J. Chem. Phys. **45**, 1469 (1966).
[6] M.E. Fisher, J. Stat. Phys. **79**, 1052 (1983).
[7] T. Dauxois, M. Peyrard, and A.R. Bishop, Phys. Rev. E **47**, R44 (1993).
[8] T. Dauxois and M. Peyrard, Phys. Rev. E **51**, 4027 (1995).
[9] M. Barbi, S. Cocco, and M. Peyrard, Phys. Lett. A **253**, 358 (1999).
[10] S. Cocco and R. Monasson, Phys. Rev. Lett. **83**, 5178 (1999).
[11] D. Cule and T. Hwa, Phys. Rev. Lett. **79**, 2375 (1997); e-print cond-mat/9701117.
[12] S. Mukherji and S. Bhattacharjee, Phys. Rev. E **48**, 3483 (1993).
[13] S. Bhattacharjee and S. Mukherji, Phys. Rev. Lett. **70**, 49 (1993); **70**, 3359(E) (1993).
[14] P. Belohorec and B. Nickel, University of Guelph report, 1997 (unpublished).
[15] S. Caracciolo, M.S. Causo, and A. Pelissetto, Phys. Rev. E **57**, R1215 (1998).
[16] E. Eisenriegler, K. Kremer, and K. Binder, J. Chem. Phys. **77**, 6296 (1982).
[17] R. Hegger and P. Grassberger, J. Phys. A **27**, 4069 (1994).
[18] H.W. Diehl, in *Phase Transitions and Critical Phenomena*, edited by C. Domb and J.L. Lebowitz (Academic Press, New York, 1986), Vol. 10.
[19] P. Pfeuty, D. Jasnow, and M. Fisher, Phys. Rev. B **10**, 2088 (1974).
[20] R.R. dos Santos and R.B. Stinchcombe, J. Phys. A **14**, 2741 (1981).
[21] B. Derrida and H.J. Herrmann, J. Phys. (Paris) **44**, 1365 (1983).
[22] N.B. Wilding and A.D. Bruce, J. Phys.: Condens. Matter **4**, 3087 (1992).
[23] N.B. Wilding, M. Müller, and K. Binder, J. Chem. Phys. **105**, 802 (1996).
[24] A.M. Ferrenberg and R.H. Swendsen, Phys. Rev. Lett. **61**, 2635 (1988); **63**, 1195 (1989).
[25] P. Grassberger, Phys. Rev. E **56**, 3682 (1997).
[26] M.N. Rosenbluth and A.W. Rosenbluth, J. Chem. Phys. **23**, 356 (1955).
[27] H. Frauenkron, M.S. Causo, and P. Grassberger, Phys. Rev. E **59**, R16 (1999).

[28] S. Caracciolo, M.S. Causo, P. Grassberger, and A. Pelissetto, J. Phys. A **32**, 2931 (1999).
[29] P. Grassberger, J. Chem. Phys. **111**, 440 (1999).
[30] T. Garel, H. Orland, and E. Orlandini, e-print cond-mat/9902147.
[31] J. des Cloizeaux and G. Jannink, *Les Polymères en Solution* (Les Editions de Physique, Les Ulis, 1987) [*Polymers in Solution: Their Modeling and Structure* (Oxford University Press, Oxford, 1990)].
[32] D.S. McKenzie and M.A. Moore, J. Phys. A **4**, L82 (1971).
[33] S. Caracciolo, M.S. Causo, and A. Pelissetto, e-print hep-lat/9910016.
[34] G.S. Joyce, in *Phase Transitions and Critical Phenomena*, edited by C. Domb and M. S. Green (Academic Press, New York, 1972), Vol. 2.